

Studying the $P_c(4450)$ resonance in J/ψ photoproduction off protons

A. N. Hiller Blin,^{1,2} C. Fernández-Ramírez,³ A. Jackura,^{2,4}
 V. Mathieu,^{2,4} V. I. Mokeev,⁵ A. Pilloni,^{5,6} and A. P. Szczepaniak^{2,5,4}
 (Joint Physics Analysis Center)

¹*Departamento de Física Teórica and IFIC, Centro Mixto Universidad de Valencia-CSIC, Institutos de Investigación de Paterna, E-46071 Valencia, Spain*

²*Center for Exploration of Energy and Matter, Indiana University, Bloomington, IN 47403, USA*

³*Instituto de Ciencias Nucleares, Universidad Nacional Autónoma de México, Ciudad de México 04510, Mexico*

⁴*Physics Department, Indiana University, Bloomington, IN 47405, USA*

⁵*Thomas Jefferson National Accelerator Facility, Newport News, VA 23606, USA*

⁶*INFN Sezione di Roma, Roma, I-00185, Italy*

(Dated: June 30, 2016)

A resonance-like structure, the $P_c(4450)$, has recently been observed in the $J/\psi p$ spectrum by the LHCb collaboration. We discuss the feasibility of detecting this structure in J/ψ photoproduction in the CLAS12 experiment at JLab. We present a first estimate of the upper limit for the branching ratio of the $P_c(4450)$ to $J/\psi p$. Our estimates, which take into account the experimental resolution effects, predict that it will be possible to observe a sizable cross section close to the J/ψ production threshold and shed light on the $P_c(4450)$ resonance in the future photoproduction measurements.

PACS numbers: 13.30.Eg, 14.20.Pt, 25.20.Lj

I. INTRODUCTION

Exotic hadron spectroscopy opens a new window into quark-gluon dynamics that could shift the paradigm that mesons and baryons consist of $q\bar{q}$ and qqq constituent quarks, respectively. Recent lattice QCD studies of the nucleon spectrum indicate that the excited nucleon states may exist with a substantial admixture of glue [1]. These recent predictions initiated the efforts aimed at a search for hybrid baryons in the future experiments at Jefferson Lab with the CLAS12 detector [2, 3]. In this paper we discuss the feasibility of using the CLAS12 detector in search for exotic baryons with the quark core consisting of five constituent quarks including charm. This is motivated by Refs. [4–6], where the authors propose to use photons to produce hidden-charm pentaquarks of the type that were reported by the LHCb collaboration in the $\Lambda_b^0 \rightarrow K^-(J/\psi p)$ channel [7]. In the LHCb data, two structures were observed, the broader has a width of $205 \pm 18 \pm 86$ MeV and mass $4380 \pm 8 \pm 29$ MeV, and the narrower has width $39 \pm 5 \pm 19$ MeV and mass $4449.8 \pm 1.7 \pm 2.5$ MeV. The preferred spin-parity assignment of these structures is that of $J_r = 3/2$ or $J_r = 5/2$ and opposite parities. Here we focus on the narrower structure, referred to as $P_c(4450)$, since we expect the broad one to be more susceptible to variations in the analysis model used to describe the coherent background. Various interpretations of these structures have been proposed. The possibility of a loosely-bound molecular state of charmed baryons and mesons was investigated in [8–12], while a resonance interpretation in terms of quark degrees of freedom was proposed in [13–16]. The possibility that these structures are nonresonant, for example due to the presence of nearby singularities in cross channels was discussed in [17–20] (for recent reviews on the

exotic charmonium-like sector, see [21]). If the resonant nature holds, it would be the first time that a signature of a hidden-charm baryon state is found. It is therefore important to look for other ways to produce the $J/\psi p$ system near threshold [4–6]. For example, if a peak in the $J/\psi p$ mass spectrum appears in photoproduction, the nonresonant interpretation of the LHCb result would be less likely.

In this paper we make a prediction for the J/ψ photoproduction cross section measurement for the CLAS12 experiment at JLab. We closely follow the arguments of [5], in particular for the application of vector-meson dominance (VMD). To describe the baryon-resonance photoproduction we use the model of [22] that was successfully applied in the past to the analysis of N^* photo- and electroproduction in the exclusive $\pi^+\pi^-p$ channel. Compared to hadronic production, the exclusive J/ψ photoproduction off protons is expected to have a large $P_c(4450)$ resonant contribution relative to the background. Furthermore, unlike the LHCb case, there is no “third” particle in the final state that the $J/\psi p$ system could rescatter from. The existing photoproduction data [23–25] mainly cover the range of photon energies above 100 GeV, *i.e.* well above the possible resonance signal, and it can be well understood as diffractive production. The few data points in the energy range of interest [26] have a mass resolution which is too low to identify a potential resonance signal. The LHCb peak in photoproduction is expected in a photon energy range where the diffractive cross section is rather low and one can expect a clearly visible resonance peak.

The CLAS12 detector is replacing the CLAS apparatus in Hall B at JLab and was optimized for measurements of nucleon resonances in electro- and photoproduction via decays to several exclusive meson-nucleon final states [27]. The excitation of the possible hidden charm

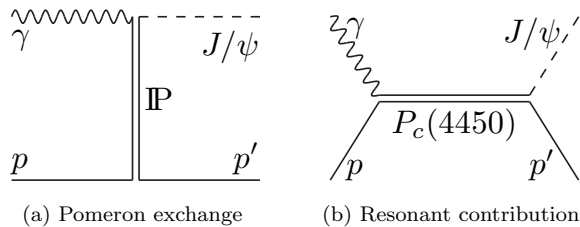


FIG. 1. Dominant contributions to the J/ψ photoproduction. The nonresonant background is modeled by an effective Pomeron exchange (a) while the resonant contribution of the $P_c(4450)$ in the direct channel (b) is modeled by a Breit-Wigner amplitude.

resonance in the $J/\psi p$ system requires photons with energies up to 11 GeV, and the identification of the resonance involves partial wave analysis. Therefore the measurement of the differential cross section and spin-density matrix elements would be desired. The cross section measurement will be possible with the data from the forward tagger built into the new CLAS12 detector. Ultimately, if the resonance signal is found, it would be of interest to extend the present study to $J/\psi p$ electroproduction, to investigate its internal structure. The J/ψ -polarization information is currently not feasible with CLAS12 without muon detection capability, but if the signal is found it would be a good candidate for a detector upgrade.

II. REACTION MODEL

A. Resonant contribution

The processes contributing to $\gamma p \rightarrow J/\psi p$ are shown in Fig. 1. The nonresonant background is expected to be dominated by the t -channel Pomeron exchange, and we saturate the s -channel by the $P_c(4450)$ resonance. In the

following we consider only the most favored $J_r^P = 3/2^-$ and $5/2^+$ spin-parity assignments for the resonance. We adopt the usual normalization conventions [28], and express the differential cross section in terms of the helicity amplitudes $\langle \lambda_\psi \lambda_{p'} | T_r | \lambda_\gamma \lambda_p \rangle$,

$$\frac{d\sigma}{d\cos\theta} = \frac{4\pi\alpha}{32\pi s} \frac{p_f}{p_i} \frac{1}{4} \sum_{\lambda_\gamma, \lambda_p, \lambda_\psi, \lambda_{p'}} |\langle \lambda_\psi \lambda_{p'} | T_r | \lambda_\gamma \lambda_p \rangle|^2. \quad (1)$$

Here, p_i and p_f are the incoming and outgoing center-of-mass frame momenta, respectively, θ is the center-of-mass scattering angle, and $W = \sqrt{s}$ is the invariant mass.

Note that the electric charge $\sqrt{4\pi\alpha}$ is explicitly factored out from the matrix element. The contribution of the $P_c(4450)$ resonance is parametrized using the Breit-Wigner ansatz [22],

$$\langle \lambda_\psi \lambda_{p'} | T_r | \lambda_\gamma \lambda_p \rangle = \frac{\langle \lambda_\psi \lambda_{p'} | T_{\text{dec}} | \lambda_R \rangle \langle \lambda_R | T_{\text{em}}^\dagger | \lambda_\gamma \lambda_p \rangle}{M_r^2 - W^2 - i\Gamma_r M_r}. \quad (2)$$

The numerator is given by the product of photoexcitation and hadronic decay helicity amplitudes. The measured width is narrow enough to be approximated with a constant, $\Gamma_r = (39 \pm 24)$ MeV. The angular momentum conservation restricts the sum over λ_R , the spin projection along the beam direction in the center of mass frame, to $\lambda_R = \lambda_\gamma - \lambda_p$. The hadronic helicity amplitude T_{dec} , which represents the decay of the resonance of spin J to the $J/\psi p$ state, is given by

$$\langle \lambda_\psi \lambda_{p'} | T_{\text{dec}} | \lambda_R \rangle = g_{\lambda_\psi \lambda_{p'}} d_{\lambda_R, \lambda_\psi - \lambda_{p'}}^J(\cos\theta), \quad (3)$$

where $g_{\lambda_\psi \lambda_{p'}}$ are the helicity couplings between the resonance and the final state. There are three independent couplings with $\lambda_{p'} = \frac{1}{2}$, $\lambda_\psi = \pm 1, 0$, being the other three related by parity. For simplicity, we assume all these couplings to be equal, *i.e.* $g_{\lambda_\psi \lambda_{p'}} \equiv g$. The helicity amplitudes and the partial decay width $\Gamma_{\psi p}$ are related by

$$\Gamma_{\psi p} = \mathcal{B}_{\psi p} \Gamma_r = \frac{\bar{p}_f}{32\pi^2 M_r^2} \frac{1}{2J_r + 1} \sum_{\lambda_R} \int d\Omega |\langle \lambda_\psi \lambda_{p'} | T_{\text{dec}} | \lambda_R \rangle|^2 = \frac{\bar{p}_f}{8\pi M_r^2} \frac{6g^2}{2J_r + 1}, \quad (4)$$

with $\mathcal{B}_{\psi p}$ being the branching ratio of $P_c \rightarrow J/\psi p$ and \bar{p}_f the momentum p_f evaluated at the resonance peak. We assume that the $P_c(4450)$ decay is dominated by the lowest partial wave, with angular momentum $\ell = 0$ for $J_r^P = 3/2^-$ and $\ell = 1$ for $J_r^P = 5/2^+$. We recall that the following near-threshold behavior of the helicity amplitudes holds: $g \propto p_f^\ell$.

The helicity matrix elements of T_{em} are usually parametrized in terms of two independent coupling constants, $A_{1/2}$ and $A_{3/2}$, which are related to the matrix

elements with $\lambda_R = 1/2, 3/2$, respectively. The other two helicities $-1/2$ and $-3/2$ are constrained by parity. Using the standard normalization convention, in which the helicity couplings A_{λ_R} have units of $\text{GeV}^{-1/2}$ and are proportional to the unit electromagnetic charge,

$$\langle \lambda_\gamma \lambda_p | T_{\text{em}} | \lambda_R \rangle = \frac{W}{M_r} \sqrt{\frac{8M_N M_r \bar{p}_i}{4\pi\alpha}} \sqrt{\frac{\bar{p}_i}{p_i}} A_{1/2, 3/2}, \quad (5)$$

with \bar{p}_i the momentum p_i evaluated at the resonance

peak. The electromagnetic decay width Γ_γ is given by

$$\Gamma_\gamma = \frac{\bar{p}_i^2}{\pi} \frac{2M_N}{(2J_r + 1)M_r} \left[|A_{1/2}|^2 + |A_{3/2}|^2 \right]. \quad (6)$$

B. Vector meson dominance

The photon helicity amplitudes for a pentaquark are not known. To rely on data as much as possible, we start by following Ref. [5] and assume a VMD relation for the transverse vector-meson helicity amplitudes

$$\langle \lambda_\gamma \lambda_p | T_{\text{em}} | \lambda_R \rangle = \frac{\sqrt{4\pi\alpha} f_\psi}{M_\psi} \langle \lambda_\psi = \lambda_\gamma, \lambda_p | T_{\text{dec}} | \lambda_R \rangle, \quad (7)$$

with f_ψ being the J/ψ decay constant which is proportional to the electromagnetic current matrix elements, $\langle 0 | J_{\text{em}}^\mu(0) | J/\psi(p, \lambda) \rangle = \sqrt{4\pi\alpha} f_\psi M_\psi e^\mu(p, \lambda)$. The decay constant is related to the J/ψ wave function via the Van Royen-Weisskopf relation, and can be estimated from the leptonic decay width of the $J/\psi \rightarrow l^+ l^-$, yielding $f_\psi = 280$ MeV.

Finally, the VMD leads to

$$\Gamma_\gamma = 4\pi\alpha \Gamma_{\psi p} \left(\frac{f_\psi}{M_\psi} \right)^2 \left(\frac{\bar{p}_i}{\bar{p}_f} \right)^{2\ell+1} \times \frac{4}{6}, \quad (8)$$

with the factor 4/6 due to the fact that in Eq. (7) only the transverse polarizations of the J/ψ contribute. Again, we use $\ell = 0$ for $J_r^P = 3/2^-$ and $\ell = 1$ for $J_r^P = 5/2^+$.

With the help of Eqs. (6) and (8), one can constrain the size of the photocouplings.

C. Nonresonant contribution

The background in the resonance region is assumed to be dominated by diffractive production, which we

TABLE I. Parameters of the fits with $P_c(4450)$ incorporated as a spin-3/2 resonance. Uncertainties in the parameters are provided at a 1σ (68%) CL except for the branching ratio $\mathcal{B}_{\psi p}$, whose upper limits are provided at a 95% CL. The first line provides the smearing applied to the three lowest-energy experimental data points in Fig. 2.

σ_s (MeV)	0	60	120
A	$0.156^{+0.029}_{-0.020}$	$0.157^{+0.039}_{-0.021}$	$0.157^{+0.037}_{-0.022}$
α_0	$1.151^{+0.018}_{-0.020}$	$1.150^{+0.018}_{-0.026}$	$1.150^{+0.015}_{-0.023}$
α' (GeV $^{-2}$)	$0.112^{+0.033}_{-0.054}$	$0.111^{+0.037}_{-0.064}$	$0.111^{+0.038}_{-0.054}$
s_t (GeV 2)	$16.8^{+1.7}_{-0.9}$	$16.9^{+2.0}_{-1.6}$	$16.9^{+2.0}_{-1.1}$
b_0 (GeV $^{-2}$)	$1.01^{+0.47}_{-0.29}$	$1.02^{+0.61}_{-0.32}$	$1.03^{+0.49}_{-0.31}$
$\mathcal{B}_{\psi p}$ (95% CL)	$\leq 29\%$	$\leq 30\%$	$\leq 23\%$

parametrize by an effective, helicity-conserving, Pomeron exchange model [29],

$$\langle \lambda_\psi \lambda_{p'} | T_P | \lambda_\gamma \lambda_p \rangle = iA \left(\frac{s - s_t}{s_0} \right)^{\alpha(t)} e^{b_0(t - t_{\text{min}})} \delta_{\lambda_p \lambda_{p'}} \delta_{\lambda_\psi \lambda_\gamma}. \quad (9)$$

Here $s_0 = 1$ GeV 2 is fixed. Frequently s_0 is chosen to match the average s of an experiment and that leads to different values for the slope parameter. This is unphysical. The physical value of s_0 is determined by the range of interactions in the s -channel, which should be of the order of the hadronic scale. The Pomeron trajectory is given by $\alpha(t) = \alpha_0 + \alpha' t$, where α_0 and α' are parameters to be determined, as well as the normalization A , the effective threshold parameter s_t , and the t -slope parameter b_0 .

There seems to be a rapid decrease of the cross section in the threshold region and the shift parameter s_t is introduced to enable a smooth connection between the high energy, $W \sim \mathcal{O}(100$ GeV), and the threshold.

III. RESULTS

To the best of our knowledge, there is no estimate for the upper limit of the branching ratio of the $P_c \rightarrow J/\psi p$ decay. To do so, we aim to fit available data on differential cross sections $d\sigma(\gamma p \rightarrow J/\psi p)/dt$ with our model given by the coherent sum of the two amplitudes: T_P for the nonresonant Pomeron background and T_r for the resonance.

The most recent and accurate data for this reaction come from the ZEUS [24] and H1 [25] experiments, with a photon energy in the laboratory frame $E_\gamma \gtrsim 200$ GeV. We use the data points with $|t| \leq 1.5$ GeV 2 to constrain the Pomeron parameters. For the low-energy region, we use data from Camerini *et al.* [23], collected at SLAC, that cover the $E_\gamma \sim 13$ –22 GeV energy range. To further constrain the fit, we consider the two lowest-energy data

TABLE II. Parameters of the fits with $P_c(4450)$ incorporated as a spin-5/2 resonance. Uncertainties in the parameters are provided at a 1σ (68%) CL except for the branching ratio $\mathcal{B}_{\psi p}$, whose upper limits are provided at a 95% CL. The first line provides the smearing applied to the three lowest-energy experimental data points in Fig. 2.

σ_s (MeV)	0	60	120
A	$0.152^{+0.032}_{-0.024}$	$0.150^{+0.043}_{-0.034}$	$0.150^{+0.044}_{-0.041}$
α_0	$1.154^{+0.020}_{-0.020}$	$1.156^{+0.027}_{-0.028}$	$1.156^{+0.033}_{-0.028}$
α' (GeV $^{-2}$)	$0.120^{+0.064}_{-0.052}$	$0.125^{+0.076}_{-0.089}$	$0.126^{+0.077}_{-0.105}$
s_t (GeV 2)	$16.6^{+1.6}_{-1.1}$	$16.6^{+2.2}_{-1.5}$	$16.6^{+2.1}_{-2.0}$
b_0 (GeV $^{-2}$)	$0.95^{+0.51}_{-0.51}$	$0.90^{+0.85}_{-0.65}$	$0.90^{+1.00}_{-0.69}$
$\mathcal{B}_{\psi p}$ (95% CL)	$\leq 17\%$	$\leq 12\%$	$\leq 8\%$

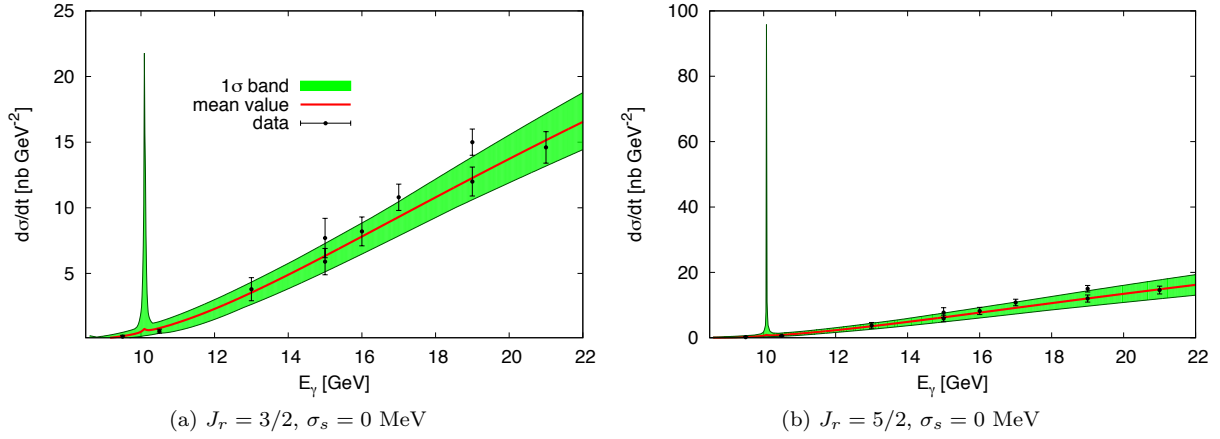


FIG. 2. Comparing data (solid circles) with the fit results at a 1σ (68%) CL, as discussed in the text, for near-threshold differential cross section data [23, 26] in the forward direction. For the cases shown in this figure, no smearing due to experimental resolution is performed.

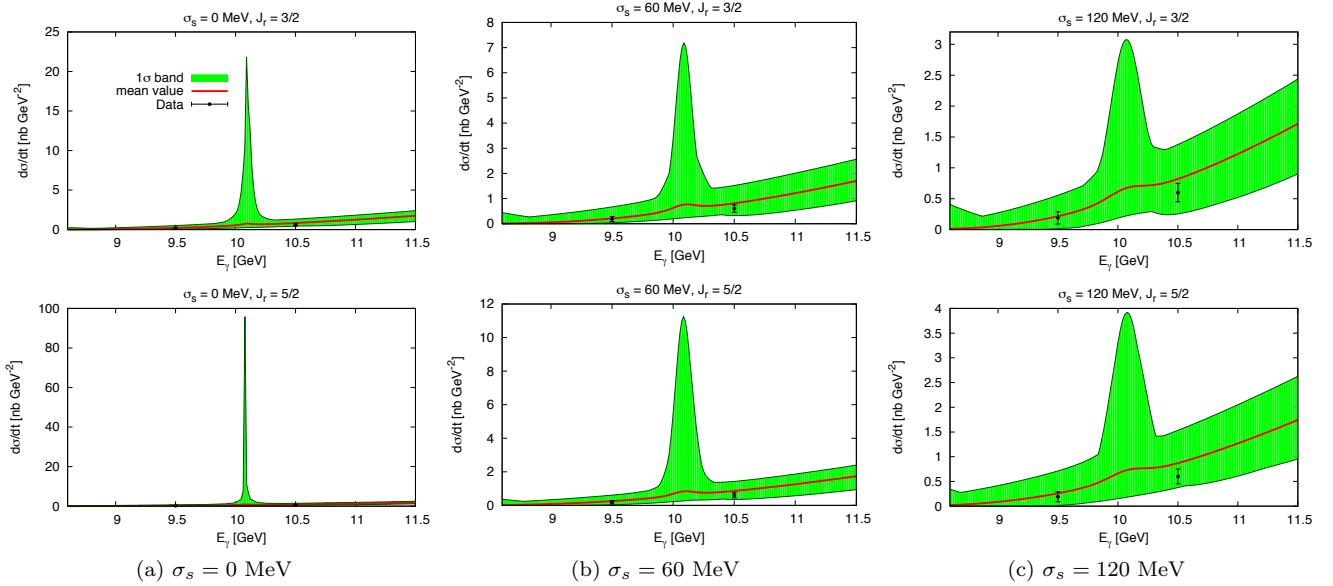


FIG. 3. Comparing data (circles) with the fit results at a 1σ (68%) CL, as discussed in the text, for near-threshold differential cross section data [23, 26] in the forward direction. Note that the vertical axes have different scales.

TABLE III. Upper limits at the 2σ (95%) CL for the resonance parameters obtained for the two J_r^P assignments. We consider three possible values for the experimental resolution σ_s . The resulting values for g follow from Eq. (4) and the photocouplings $A_{1/2}$ and $A_{3/2}$ are determined using VMD and assuming the couplings to be of equal size for the different helicity combinations.

J_r^P	$3/2^-$			$5/2^+$		
σ_s (MeV)	0	60	120	0	60	120
$\mathcal{B}_{\psi p}$	$\leq 29\%$	$\leq 30\%$	$\leq 23\%$	$\leq 17\%$	$\leq 12\%$	$\leq 8\%$
g (GeV)	≤ 2.1	≤ 2.2	≤ 1.9	≤ 2.0	≤ 1.5	≤ 1.4
Γ_γ (keV)	≤ 14.4	≤ 14.9	≤ 11.0	≤ 56.9	≤ 33.5	≤ 26.8
$A_{1/2,3/2}$ ($\text{GeV}^{-1/2}$)	≤ 0.007	≤ 0.007	≤ 0.006	≤ 0.017	≤ 0.013	≤ 0.012
$\frac{d\sigma}{dt} _{E_\gamma=E_r, t=t_{\min}}$ (nb GeV^{-2})	≤ 21.8	≤ 7.2	≤ 3.1	≤ 95.8	≤ 11.3	≤ 3.9
$\sigma_{\text{tot}} _{E_\gamma=E_r}$ (nb)	≤ 120	≤ 38	≤ 14	≤ 396	≤ 44	≤ 14

points shown in SLAC preprints [26], right across the pentaquark peak. In total, we consider 137 $\gamma p \rightarrow J/\psi p$ data points for the $d\sigma(\gamma p \rightarrow J/\psi p)/dt$ differential cross sections, with $|t| \leq 1.5 \text{ GeV}^2$, covering energy ranges from threshold to $E_\gamma \sim 120 \text{ TeV}$ in the lab frame.

To compare with the data it is necessary to consider effects of experimental resolution, mainly due to the uncertainty in photon energy. We introduce a smearing in the calculation of the observables, by convoluting the theoretical cross section with a Gaussian distribution

$$G(x) = \frac{\exp(-x^2/2\sigma_s^2)}{\sqrt{2\pi}\sigma_s}, \quad (10)$$

where σ_s is the smearing. The convolution is then given by introducing this function into

$$\frac{d\sigma}{d\Omega} \rightarrow \left(\frac{d\sigma}{d\Omega} * G \right) (E_\gamma) = \int_{-\infty}^{\infty} \frac{d\sigma}{d\Omega}(y) G(E_\gamma - y) dy, \quad (11)$$

where E_γ is the photon energy in the laboratory frame. All the parameters of the model are treated as free parameters in our fits, *i.e.*, the $P_c(4450) \rightarrow J/\psi p$ branching ratio $\mathcal{B}_{\psi p}$ and the Pomeron parameters: A , α_0 , α' , s_t and b_0 . Only the three lowest-energy data with $t = t_{\min}$ (see Fig. 2) have been smeared with the experimental resolution.

The mean value of the parameters and the uncertainties have been computed employing the bootstrap technique [31]. The bootstrap technique allows to take into account the correlations among parameters and to properly propagate their uncertainties to the observables [32]. The procedure is as follows. First we explored the parameter space with 10^5 fits using MINUIT [33] in order to identify the region where the absolute minimum lies. The starting values of the parameters were randomly selected in a very wide range. Once the parameter-space region where the absolute minimum lies has been identified, we use this information to randomly seed the starting values of the parameters for our fits. We generate 10^4 data sets for each one of the two J_r^P options ($3/2^-$ and $5/2^+$) and three smearings ($\sigma_s = 0, 60, \text{ and } 120 \text{ MeV}$) by randomly sampling the experimental points and the pentaquark mass and width according to their uncertainties. The mass of the $P_c(4450)$ ($M_r = 4449.8 \pm 3.2 \text{ MeV}$) is sampled according to a Gaussian distribution, while the width, in order to avoid negative values, is sampled according to a Gamma distribution

$$H(x | \Gamma_r, \sigma_r) = \left(\frac{x \Gamma_r}{\sigma_r^2} \right)^{\frac{\Gamma_r}{\sigma_r^2}} \frac{\exp(-x \Gamma_r / \sigma_r^2)}{x \Gamma(\Gamma_r / \sigma_r^2)}, \quad (12)$$

where $\Gamma_r = 39 \text{ MeV}$ is the pentaquark width and $\sigma_r = 24 \text{ MeV}$ its uncertainty. The experimental data point with the lowest photon energy and $t = t_{\min}$ (see Figs. 2 and 3) is also sampled according to a Gamma distribution to avoid a negative value of the differential cross section, while the rest of the experimental data points are

sampled according to Gaussian distributions. For each data set, an independent Maximum Likelihood Fit is performed using MINUIT [33]. For each smearing option, once the 10^4 data sets have been fitted, we can extract the best 68% fits, whose mean value for each parameter provides the best values reported in Tables I and II and the upper and lower values for each parameter provide the uncertainties. With this set of parameters that correspond to 1σ confidence level (CL) we can compute each observable and its uncertainty [31]. Computing quantities at a any other CL (*e.g.* 2σ) can be achieved in the same way, given that enough fits are computed. Figure 3 shows the results of the fits for the different smearing parameters. We also show the high-energy data compared to our fit result for the case of no smearing in Fig. 4.

Since there are no data for the resonance peak and there is no known lower limit for the branching fraction, the mean values of the parameters are naturally consistent with the non existence of the $P_c(4450)$. We find that the upper limit for the branching ratio $\mathcal{B}_{\psi p}$ at a 95% CL ranges from 23% to 30% for $J_r = 3/2$, depending on the experimental resolution, and from 8% to 17% for $J_r = 5/2$. The resulting hadronic couplings, as well as the photocouplings, are summarized in Table III. It is worth noting that A is highly correlated with α_0 , α' and b_0 are also highly correlated, and that s_t is correlated with A and b_0 . $\mathcal{B}_{\psi p}$ is equally correlated with all the parameters.

It is possible that a structure at 10 GeV had indeed not been seen in the past, because of the finite resolution as the peak strength decreases and becomes broader and flatter. Its detection requires finer energy binning. The peak is expected to be narrow, falling in between two bins where data is available. Therefore, it is important to perform an energy scan in this region to confirm the existence of the resonance.

While there are no data on the angular dependence near threshold yet, we can make a few predictions based on the model presented above. In order to be able to do a deeper study of this dependence, we now relax the VMD condition and let the relative sizes of the photocouplings vary. As expected, the results depend on the relative size of the helicity amplitudes, as shown in Fig. 5 for three different cases $A_{1/2} = A_{3/2}$, $A_{3/2} = 0$, and $A_{1/2} = 0$, while maintaining the sum of the squares $|A_{1/2}|^2 + |A_{3/2}|^2$ constant. Pronounced differences in the predicted angular distributions under different assignments for the $P_c(4450)$ photocouplings and spins demonstrate the prospect of determining these quantities from the future experimental data on J/ψ photoproduction cross sections measured with CLAS12 in the near-threshold region.

Finally, we discuss the results for the total cross section, shown in Fig. 6 for the two possible spin assignments $3/2$ and $5/2$, and the different experimental resolutions shown in Tabs. I to III. The resonant piece of the resulting cross section is consistent with the one predicted by Ref. [5] when taking the same spin and branching-ratio assumptions: $J_r = 3/2$ and $\mathcal{B}_{\psi p} = 10\%$.

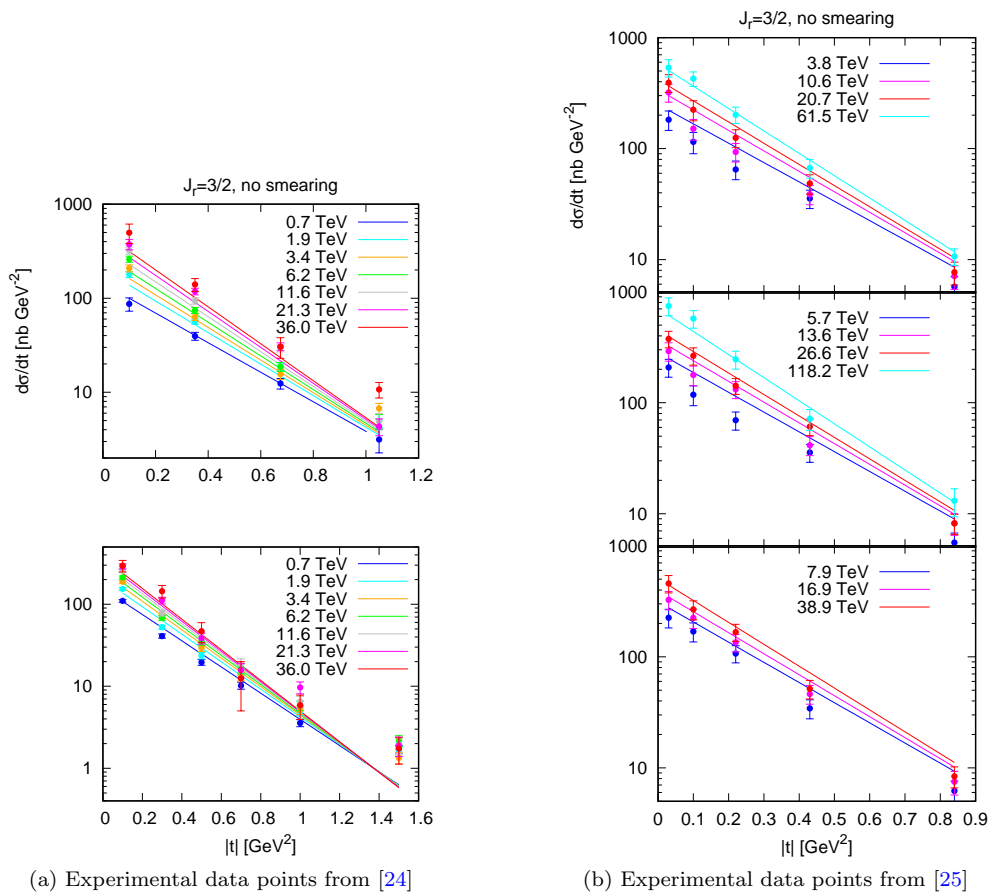


FIG. 4. Comparing data (circles) with the fit-results' mean values, for $J_r^P = 3/2^-$, and $\sigma_s = 0$ MeV, and different values of incoming photon energy in the lab frame. The error bands are not shown here to ease the plot reading.

IV. SUMMARY

We studied the possibility of observing the $P_c(4450)$ resonance in J/ψ photoproduction at CLAS12. The data available in this energy range are scarce and there is no measurement of the differential cross section. We tested the compatibility of the data and a simple two-component model containing the directly produced resonance and a diffractive background. We conclude that, the resonance peak being narrow enough, it could have escaped detection due to poor energy resolution.

From the fits to the available J/ψ photoproduction data, we show that the magnitude of the peak for the $P_c(4450)$ resonance can range from very strong to barely visible. Our results demonstrate the possibility to observe the $P_c(4450)$ resonance and to determine its spin and photocouplings. Therefore, the future data on J/ψ photoproduction off protons measured in the near threshold region with a quasi-real photon beam at JLab will allow us to explore photoexcitation of the $P_c(4450)$ state suggested by LHCb data.

We made a prediction for the angular distribution which can be used to disentangle the spin of the resonance and helicity dependence of the resonance production. If the resonance signal is found, photon-virtuality dependence can be used to investigate the resonance structure.

ACKNOWLEDGMENTS

This material is based upon work supported in part by the U.S. Department of Energy, Office of Science, Office of Nuclear Physics under contracts DE-AC05-06OR23177 and DE-FG0287ER40365, National Science Foundation under grants PHY-1415459 and NSF-PHY-1205019, and IU Collaborative Research Grant. This work was also supported by the Spanish Ministerio de Economía y Competitividad (MINECO) and European FEDER funds under contract No. FIS2014-51948-C2-2-P and SEV-2014-0398. ANHB acknowledges support from the Santiago Grisolia program of the Generalitat Valenciana and from the Center for Exploration of Energy and Matter at Indiana University.

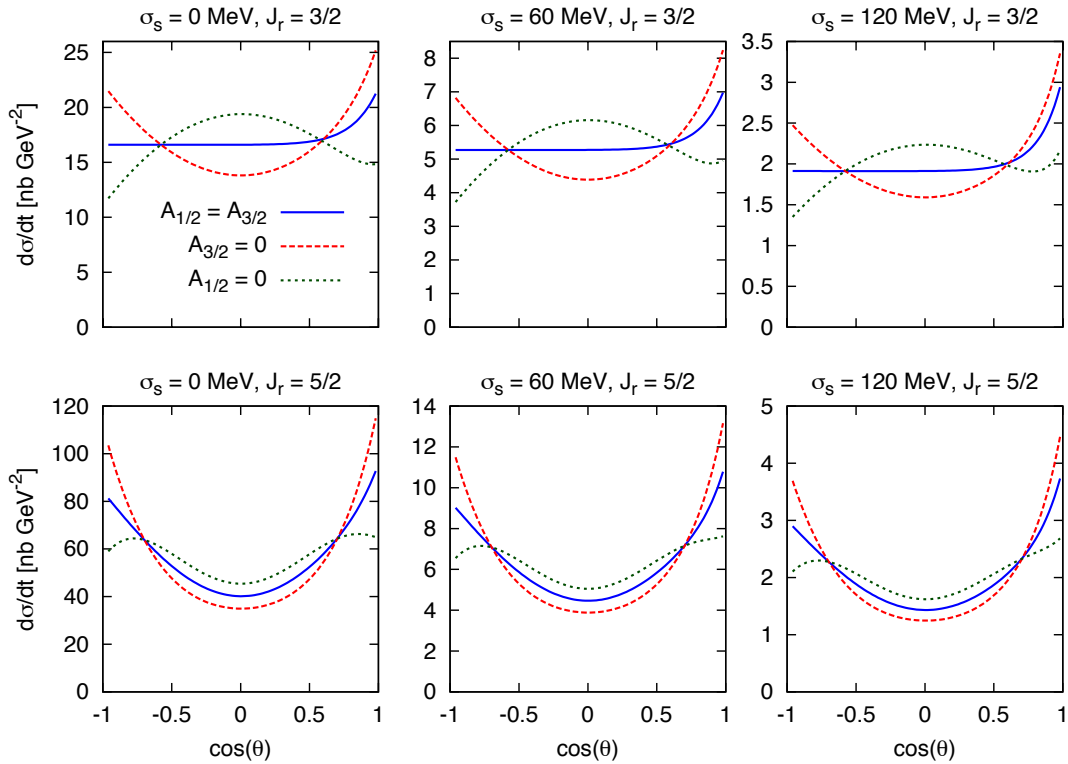


FIG. 5. Theoretical curves for the differential cross section angular distribution at the resonance energy. We present the results for the 95% CL upper limits for the branching ratio values, as shown in Tables I and II for two $P_c(4450)$ spin possibilities and three different photocoupling settings: $A_{1/2} = A_{3/2}$ (solid blue); $A_{3/2} = 0$ (dashed red); $A_{1/2} = 0$ (dotted green).

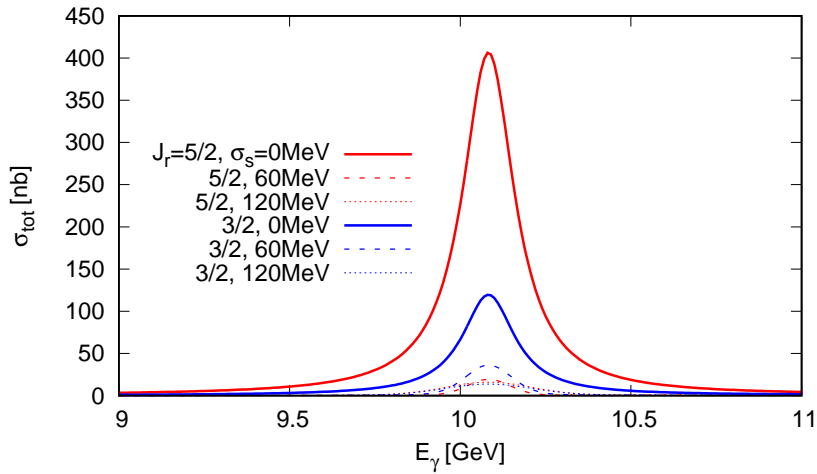


FIG. 6. The expected total J/ψ photoproduction cross section in the $P_c(4450)$ resonance region, as a function of the lab-frame photon energy E_γ . The chosen photocouplings are $A_{3/2} = A_{1/2}$ and it is evaluated at a set of fitting parameters where the branching ratio reaches its upper limit, see Tables I and II.

- [1] R. G. Edwards, N. Mathur, D. G. Richards, and S. J. Wallace (Hadron Spectrum Collaboration), Phys. Rev. D **87**, 054506 (2013), [arXiv:1212.5236 [hep-ph]].
- [2] CLAS Collaboration, *CLAS12 Technical Design Report*

- (2008), https://www.jlab.org/Hall-B/clas12_tdr.pdf.
- [3] V. D. Burkert, arXiv:1603.00919 [nucl-ex]; V. D. Burkert *et al.*, <https://www.jlab.org/exp-prog/PACpage/PAC44>.

- [4] Q. Wang, X. H. Liu, and Q. Zhao, Phys. Rev. D **92**, 034022 (2015), [[arXiv:1508.00339 \[hep-ph\]](#)].
- [5] M. Karliner and J. L. Rosner, Phys. Lett. B **752**, 329 (2016), [[arXiv:1508.01496 \[hep-ph\]](#)].
- [6] V. Kubarovsky and M. B. Voloshin, Phys. Rev. D **92**, 031502 (2015), [[arXiv:1508.00888 \[hep-ph\]](#)].
- [7] R. Aaij *et al.* (LHCb Collaboration), Phys. Rev. Lett. **115**, 072001 (2015), [[arXiv:1507.03414 \[hep-ex\]](#)]; unresolved structures also appear in the Cabibbo suppressed channel, R. Aaij *et al.* (LHCb Collaboration) [arXiv:1604.05708 \[hep-ex\]](#).
- [8] R. Chen, X. Liu, X. Q. Li, and S. L. Zhu, Phys. Rev. Lett. **115**, 132002 (2015), [[arXiv:1507.03704 \[hep-ph\]](#)].
- [9] H. X. Chen, W. Chen, X. Liu, T. G. Steele, and S. L. Zhu, Phys. Rev. Lett. **115**, 172001 (2015), [[arXiv:1507.03717 \[hep-ph\]](#)].
- [10] L. Roca, J. Nieves, and E. Oset, Phys. Rev. D **92**, 094003 (2015), [[arXiv:1507.04249 \[hep-ph\]](#)].
- [11] J. He, Phys. Lett. B **753**, 547 (2016), [[arXiv:1507.05200 \[hep-ph\]](#)].
- [12] Q.-F. Lü and Y.-B. Dong, Phys. Rev. D **93**, 074020 (2016), [[arXiv:1603.00559 \[hep-ph\]](#)].
- [13] L. Maiani, A. D. Polosa, and V. Riquer, Phys. Lett. B **749**, 289 (2015), [[arXiv:1507.04980 \[hep-ph\]](#)].
- [14] V. V. Anisovich, M. A. Matveev, J. Nyiri, A. V. Sarantsev, and A. N. Semenova, [arXiv:1507.07652 \[hep-ph\]](#).
- [15] A. Mironov and A. Morozov, JETP Lett. **102**, 271 (2015), [[arXiv:1507.04694 \[hep-ph\]](#)].
- [16] R. F. Lebed, Phys. Lett. B **749**, 454 (2015), [[arXiv:1507.05867 \[hep-ph\]](#)].
- [17] U.-G. Meißner and J. A. Oller, Phys. Lett. B **751**, 59 (2015), [[arXiv:1507.07478 \[hep-ph\]](#)].
- [18] F. K. Guo, U.-G. Meißner, W. Wang, and Z. Yang, Phys. Rev. D **92**, 071502 (2015), [[arXiv:1507.04950 \[hep-ph\]](#)].
- [19] X. H. Liu, Q. Wang, and Q. Zhao, Phys. Lett. B **757**, 231 (2016), [[arXiv:1507.05359 \[hep-ph\]](#)].
- [20] M. Mikhasenko, [arXiv:1507.06552 \[hep-ph\]](#).
- [21] H. X. Chen, W. Chen, X. Liu, and S. L. Zhu, Phys. Rept. **639**, 1 (2016) [[arXiv:1601.02092 \[hep-ph\]](#)]; A. Esposito, A. L. Guerrieri, F. Piccinini, A. Pilloni, and A. D. Polosa, Int. J. Mod. Phys. A **30**, 1530002 (2015) [[arXiv:1411.5997 \[hep-ph\]](#)].
- [22] V. I. Mokeev *et al.* (CLAS Collaboration), Phys. Rev. C **86**, 035203 (2012), [[arXiv:1205.3948 \[nucl-ex\]](#)]; V. I. Mokeev, I. Aznauryan, V. Burkert, and R. Gothe, EPJ Web Conf. **113**, 01013 (2016) [[arXiv:1508.04088 \[nucl-ex\]](#)].
- [23] U. Camerini *et al.*, Phys. Rev. Lett. **35**, 483 (1975).
- [24] S. Chekanov *et al.* (ZEUS Collaboration), Eur. Phys. J. C **24**, 345 (2002), [[hep-ex/0201043](#)].
- [25] A. Aktas *et al.* (H1 Collaboration), Eur. Phys. J. C **46**, 585 (2006), [[hep-ex/0510016](#)].
- [26] D. M. Ritson, AIP Conf. Proc. **30**, 75 (1976); R. L. Anderson, Madison Conf. 102 (1976), SLAC-PUB-1741.
- [27] I. G. Aznauryan and V. D. Burkert, Prog. Part. Nucl. Phys. **67**, 1 (2012), [[arXiv:1109.1720 \[hep-ph\]](#)]; I. G. Aznauryan, V. D. Burkert, T.-S. H. Lee, and V. I. Mokeev, J. Phys.: Conf. Ser. **299**, 012008 (2011), [[arXiv:1102.0597 \[nucl-ex\]](#)]; V. D. Burkert, Int. J. Mod. Phys. A **26**, 493 (2011), [[arXiv:1008.2809 \[nucl-ex\]](#)]; V. D. Burkert, Prog. Part. Nucl. Phys. **55**, 108 (2005); V. D. Burkert and T.-S. H. Lee, Int. J. Mod. Phys. E **13**, 108 (2004), [[nucl-ex/0407020](#)]; V. I. Mokeev *et al.*, Phys. Rev. C **93**, 025206 (2016).
- [28] K. A. Olive *et al.* (Particle Data Group), Chin. Phys. C **38**, 090001 (2014).
- [29] V. N. Gribov, Y. L. Dokshitzer, and J. Nyiri, *Strong Interactions of Hadrons at High Energies* (Cambridge University Press, Cambridge, England, 2009); V.N. Gribov, *The Theory of Complex Angular Momenta* (Cambridge University Press, Cambridge, England, 2003).
- [30] V. I. Mokeev *et al.*, Phys. Rev. C **80**, 045212 (2009), [[arXiv:0809.4158 \[hep-ph\]](#)].
- [31] W. H. Press, S. A. Teukolsky, W. T. Vetterling, and B. P. Flannery, *Numerical Recipes: The Art of Scientific Computing* (Cambridge University Press, 1992).
- [32] C. Fernández-Ramírez, I. V. Danilkin, D. M. Manley, V. Mathieu, and A. P. Szczepaniak, Phys. Rev. D **93**, 034029 (2016), [[arXiv:1510.07065 \[hep-ph\]](#)].
- [33] F. James and M. Roos, Comput. Phys. Commun. **10**, 343 (1975).